



# Assessment of mining-related seabed subsidence using GIS spatial regression methods: a case study of the Sanshandao gold mine (Laizhou, Shandong Province, China)

Jiayuan Cao<sup>1,2,3</sup> · Fengshan Ma<sup>1,2</sup> · Jie Guo<sup>1,2</sup> · Rong Lu<sup>1,2,3</sup> · Guowei Liu<sup>1,2,3</sup>

Received: 4 March 2018 / Accepted: 19 December 2018 / Published online: 2 January 2019  
© Springer-Verlag GmbH Germany, part of Springer Nature 2019

## Abstract

Land subsidence in the Sanshandao area, Laizhou, Shandong Province, China, has been a consequence of underground gold mining. This paper identifies the statistically significant mining subsidence factors, which are: (1) a digital elevation model of the surface; (2) the surface slope; (3) the slope aspect; (4) the thickness of the gold deposits; and (5) the depth of the gold deposits below the ground. The vertical displacement of the GPS monitoring in the Xishan gold mine (one of the Sanshandao gold mine) was selected as the dependent variable and five mining subsidence factors as the independent variables. Subsidence modeling was carried out in geographic information systems first with the ordinary least squares (OLS) method and then with the geographically weighted regression (GWR) method. Finally, the seabed subsidence was predicted with the geographically weighted regression model for the Xinli gold mine (another of the Sanshandao gold mine), in which the gold deposits are located under the sea. The results of the GWR analysis showed a marked improvement compared to those of the OLS analysis. The  $R^2$  value of the GWR model equals 0.82, which indicates that the model captured the spatial heterogeneity of the independent variables. The accuracy of determining subsidence in the area used for validation is  $\pm 8.5$  mm with a maximum calculated subsidence of  $-329.26$  mm. The maximum subsidence predicted with the model for the seabed is  $-63$  mm with a mean subsidence of  $-50$  mm.

**Keywords** Seabed subsidence · GIS · Spatial regression · GWR · Prediction

## Introduction

In recent years, with the deepening of the development of mineral resources, mine safety accidents caused by subsidence area of stope happened very often. Mining-related subsidence may lead to subsidence-related damages to surface infrastructure, buildings, engineering structures, farmlands, as well as interrupt the balance of underground water levels, and natural and manmade surface drainage systems (Jan

Blachowski 2016). Changes in the surface vertical direction are the main form of surface deformation in mining areas. The surface subsidence caused by mining is of limited extent, large amplitude, and can be highly destructive. Mining surface subsidence is a surface deformation phenomenon caused by changes of rock mass stress state owing to the combined action of artificial and natural factors. The depth of cover, overlying strata properties, seam thickness, panel width, chain pillar size and surface topography are the main factors used to determine the magnitude (areal extent and amount) of subsidence due to underground mining (Nestbitt 2003). Monitoring of mining surface subsidence has become a key problem that must be solved for better use of mineral resources. At present, the main methods of monitoring the mining area deformation are traditional ones, such as leveling and static GPS positioning. The main shortcomings of traditional monitoring methods are their low efficiency, vulnerability to influenced by external factors, and requirement for a large amount of manpower and material resources. In view of these shortcomings, a more efficient

✉ Fengshan Ma  
fsma@mail.iggcas.ac.cn

<sup>1</sup> Key Laboratory of Shale Gas and Geoengineering, Institute of Geology and Geophysics, Chinese Academy of Sciences, Beijing 100029, China

<sup>2</sup> Institutions of Earth Science, Chinese Academy of Sciences, Beijing 100029, China

<sup>3</sup> University of Chinese Academy of Sciences, Beijing 100049, China

and comprehensive technology for mining subsidence monitoring has been sought. Differential SAR interferometry was produced and developed from the interferometric synthetic aperture radar. The monitoring precision of this new method can reach the millimeter scale and is comparable with that of the traditional methods. Its main advantages are avoidance of the field operations, lack of influence by outside factors such as weather, monitoring of a large area, and high efficiency.

With increasing underground mining activities, the magnitude of the subsidence problem can be expected to grow in the future; thus, recent studies have focused on modeling and predicting subsidence. Empirical and phenomenological methods are usually used to predict surface subsidence (Siriwardane and Amanat 1986). Missavage et al. (1986) successfully predicted the vulnerability of shallow room and pillar mined areas to subsidence by a developed mathematical model. Satya Prakash Sahu (2017) used the multivariate statistical techniques such as factor analysis, principal component analysis, cluster analysis to assess the magnitude and extent of subsidence. Dolezalova et al. (2009, 2012) have repeatedly observed subsidence caused by underground coal mining with GPS technique and analyzed the time dependence between the mining subsidence and horizontal movements and the progress of exploitation.

This concise review shows that a large amount of work has been carried out on monitoring and modeling of mining subsidence and the related hazards for the surface and infrastructure. Because of the particularity of the mining location, assessment of mining-related seabed subsidence has become a global problem. The Sanshandao gold mine is divided into two mining areas: the Xishan gold mine, in which the ore bodies are underground and the Xinli gold mine, in which the ore bodies are located under the sea. A total of 342 GPS monitoring points were set up to monitor the land subsidence of the Xishan gold mine, so the surface deformation can easily be measured. As most of the Xinli gold mine ore bodies are under the sea, leveling, static GPS positioning and differential SAR interferometry cannot be used to assess the seabed subsidence. Assessing subsidence is important for the safety of mine production; hence, in this study, the ordinary least squares (OLS) model was first applied to develop a spatial regression model to analyze the relationships between subsidence (the dependent variable in the model) and mining subsidence factors (independent variables in the model) in the Xishan gold mine. The same set of variables was used to construct a geographically weighted regression (GWR) model. Finally, the GWR model was used to predict the seabed subsidence of the Xinli gold mine.

## Study area

### Geological setting

The Sanshandao gold mine is 25 km north of Laizhou, Shandong Province, China. The entire site is situated between longitudes  $119^{\circ}56'59''\text{E}$  and  $119^{\circ}56'59''\text{E}$  and latitudes  $37^{\circ}24'00''\text{N}$  and  $37^{\circ}24'45''\text{N}$ . It is located in the coastal zone of Laizhou. The eastern part of the area is land, and it is surrounded by the sea on three sides (Fig. 1). The area is low-lying, most of the terrain is flat, with an elevation of 1.2–4.5 m. The highest three peaks are located at the foot-wall of the F1 fault, with an elevation of about 67.3 m. The eastern part of the terrain is higher than the west, and the south is higher than the north. The Sanshandao gold mine is located at the intersection of the Jiyang depression and the Tan-Lu fault (which forms a flower structure in this area) (Wu et al. 2006). In the mining area, there are three controlling faults (F1, F2, and F3) and some typical secondary joints. Because the mining area is covered by Quaternary strata, the faults are not normally observed at the surface of the earth.

The Sanshandao gold mine is divided into two mining areas: the Xishan gold mine in the north and the Xinli gold mine in the south. The hanging side of the ore body in the Xishan gold mine is land. The earth's surface corresponding to the goaf is a densely populated area. In the distance is cultivated land and woodland. The earth's surface corresponding to the heading side of the ore body is a mountain

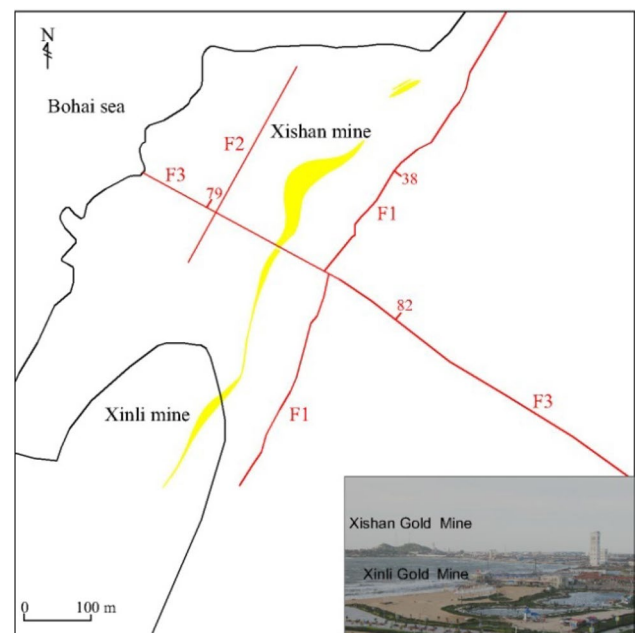


Fig. 1 Regional geological map

named Sanshan. In the distance is the sea. The Xinli gold mine is separated from the Xishan gold mine by the Wanghe River and is located in the coastal plain of Laizhou bay. The coastal area of Laizhou is a regular semidiurnal tide. The elevation of the highest tidal level (1976–2000 years) in Bohai is 2.53 m, and the lowest tide is −2.10 m. The average elevation of the sea level is +0.04 m. The Wang River flows northeast of the mine area and a few fish ponds lie in the southeast. The Wang River flows into the sea only during July and August; it is dry the rest of the year. The depth of the overlying sea water in the northwest of the mine area is about 10 m. The ore body is all under the sea. The land area of the mining region is limited and it is the only submarine deposit in China. Because of successive exploitation, the Xinli gold mine faces potential safety hazards caused by damage to the subsea surface and security isolation layer.

**Ore body occurrence and mining method**

The gold ore bodies of the two mines are altered rock type gold deposits controlled by the F1 fault (the Sanshandao–Cangshang fault). Magmatic water was formed by dehydration of mantle-derived magma. The ore bodies formed when the magmatic water ascended along the F1 fault and encountered shallow atmospheric precipitation. The ore body is located within 35 m of the principal section of the F1 fault.

Two large ore bodies are found in the Xishan gold mine, the main ore body is number I ore body and the number II ore body is the minor ore body. Number I ore body lies in the fault zone of the F1 fault. The average strike and dip angle of this ore body are 40°NE and 35–50°, respectively.

The dip direction is SE. The thickness of the ore body varies greatly, between 0.95 and 12.18 m, and the average thickness is 10.42 m. Number II ore body is located in the lower part of the northern section of the beresitization alteration belt. The average strike and the dip angle of the ore body are 43°NE and 41°, respectively. The dip direction is SE. The deposit is exploited at eleven levels (−150, −195, −240, −285, −330, −375, −420, −465, −510, −555, −600), as shown in Fig. 2 on the left.

The ore body of the Xinli gold mine is located in the footwall of the Sanshandao–Cangshang fault. The mineralization began to develop close to the main fissure, and spread in the area of the beresitization alteration belt. The average strike and the dip angle of the ore body are 52°NE and 45°, respectively. The dip direction is SE. The deposit is exploited at eleven levels (−165, −200, −240, −280, −320, −360, −400, −440, −480, −600), as shown in Fig. 2 on the right.

As the ore bodies of the two mines are controlled by the same fault, they are similar in shape. The mechanical upward horizontal slice stopping–filling method with pointed pillars is applied in both mining areas. The stope is positioned along the strike and good ventilation and drainage. The stope length is 100 m and its width is the thickness of the ore body. The strike drives used in connecting the slope ramp, ore pass, and stopes are arranged in the footwall of the ore body at 15 m intervals. The heights of the sublayer, cutting layer, and filling body are 3, 4.5, and 3 m, respectively. Horizontal cut and fill mining is adopted for some stopes. The main function of the filling body is to prevent movement of the surrounding rock, to restrict its deformation, and to change the deformation the overlying strata. However, with increasing mining depth and increasing size of the filling body, the cumulative deformation

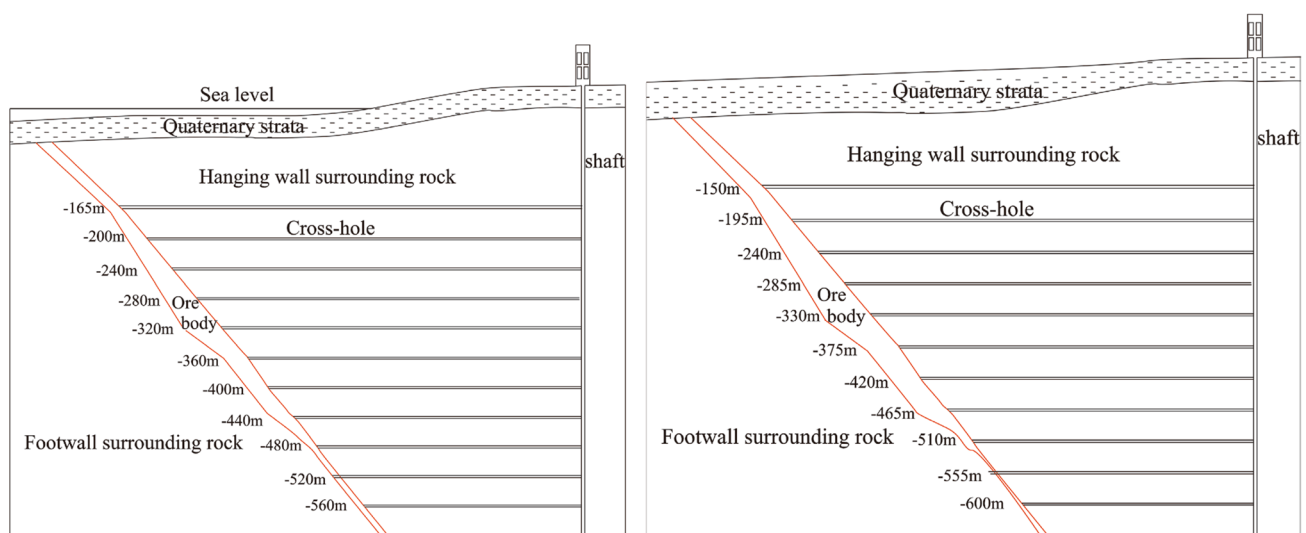


**Fig. 2** Prospecting line profile

of the filling body in an inclined mine, particularly in the case of a steep mine filling body under the influence of repeated mining and increasing crustal stress, will cause continuous movement of the overlying strata in the goaf. In the long run, this mining method can still cause large-scale rock mass movement and surface deformation.

To summarize, the Xinli and the Xishan gold mines are similar in their engineering geological conditions, ore body occurrence and mining method.

## Methodology

Spatial modeling of mining subsidence is a challenging problem due to the complexity of factors behind this process and the resulting spatial heterogeneity of variables (Jan Blachowski 2016). In GIS, ArcGIS is known for its robust spatial analysis and spatial data processing capabilities. Its spatial data processing techniques can be used to facilitate handling and processing large and numerous data sets required for subsidence modeling. In ArcGIS, the spatial relationship modeling includes two regression tools: ordinary least squares model and geographically weighted regression model. The OLS regression is a kind of simple method, its theoretical development is relatively perfect. On the basis of spatially varying-coefficient regression model, Fotheringham (1998) used local smooth thinking to propose the geographically weighted regression model. It is an extension of the normal linear regression model. It embeds the data location in the regression parameters and is a local, spatial, regression method.

The general multiple linear regression model expression is:

$$y_i = \beta_0 + \sum_{k=1}^p \beta_k \cdot x_{ki} + \varepsilon_i \quad (1)$$

where  $y_i$  is the dependent variable measured at location  $I$ ,  $x_i$  are the independent variables,  $\beta_i$  are the model coefficients,  $\varepsilon_i$  is the error,  $i = 1$  to  $p$ .

The GWR version of the OLS regression model is:

$$y_i(u) = \beta_{0i}(u) + \sum_{k=1}^p \beta_k(u) \cdot x_{ki}(u) + \varepsilon_i(u) \quad (2)$$

where  $y_i(u)$  is the dependent variable measured at location  $u$ ,  $x_{ki}(u)$  are the  $k$ TH independent variables at location  $u$ ,  $\beta_{0i}(u)$  are the model coefficients which reflect the relationship and strength of each explanatory variable to the dependent variable,  $\varepsilon_i(u)$  is the portion of the dependent variable that is not explained by the model,  $i = 1$  to  $p$ . If measurements for the independent variables  $x_{ki}(u)$  are available for the location  $u$ , then a prediction for dependent variable  $y$  may also be made.

In this study, a weighted spatial regression technique was used. The regression analysis should always begin with the OLS model, after which the GWR model is run using the same independent variables. The method was as follows. First, the important factors contributing to ground subsidence was selected as the independent variables and the vertical displacement as the dependent variable. Then, the OLS model was constructed and analyzed for the independent variables and dependent variable of the Xishan gold mine. Subsequently, a GWR model was applied to the same set of variables. Finally, a subsidence prediction map for the Xinli gold mine was produced from the GWR model.

## Analysis and discussion

### Data preparation and preprocessing

Many studies have identified important factors that contribute to ground subsidence around coal mines, including (CIPB 1997; Waltham 1989): depth and height of the mined cavities, excavation method, degree of inclination of the excavation, scope of mining, structure of the geology, flow of groundwater, and the mechanical characteristics of the rock mass rating. Taking into account geology of the mine, a digital elevation model of the surface, surface slope, slope aspect, thickness of gold deposits, and depth of gold deposits below the ground were chosen as the independent variables. All the spatial representations of independent variables were prepared as raster maps. The data layers are provided in Table 1. The final thematic maps of independent variables are shown in Fig. 3.

The vertical displacement of surface subsidence was chosen as the dependent variable. To obtain the vertical displacement, 342 monitoring points were set up in the Sanshandao gold mine from 2012, arranged along the line of the

**Table 1** Constructed GIS database including independent variables of study area

Independent variables	Remark
Digital elevation model of the surface	TIN process to get elevation data
Surface slope	Analysis of slope by ArcGIS
Slope aspect	Analysis of slope aspect by ArcGIS
Thickness of gold deposits	IDW interpolated from prospecting line profile map
Depth of gold deposits below the ground	IDW interpolated from prospecting line profile map

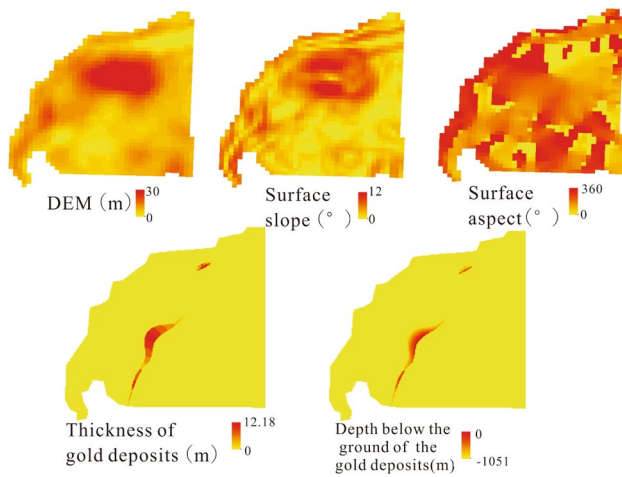
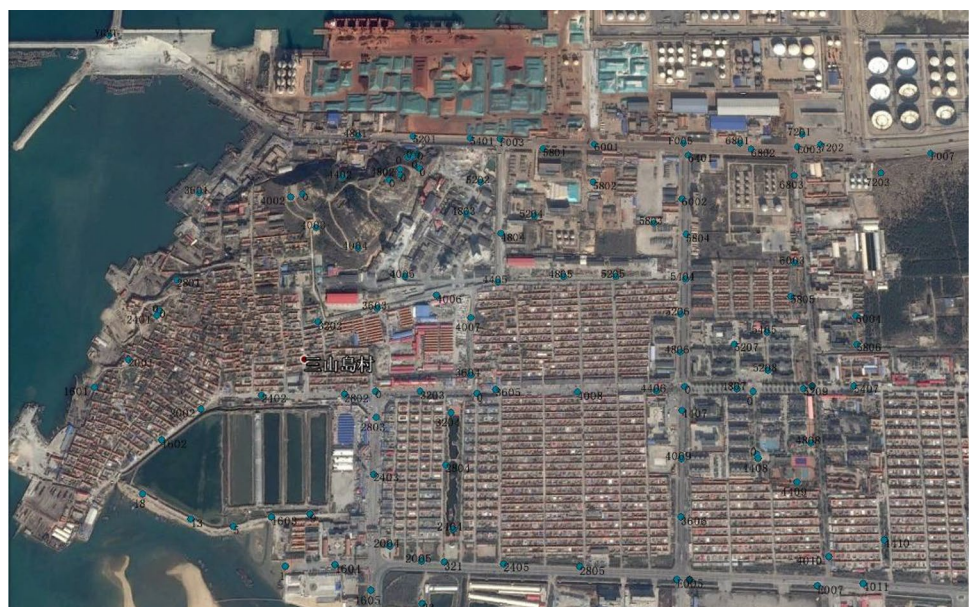


**Fig. 3** Spatial representation of independent variables in the GWR models

exploration section. The distribution of monitoring points in the Xishan gold mine is shown in Fig. 4. The GPS instrument used in this study is a Z-surveyor receiver produced by Ashtech Company, United States. It uses three receivers and the sampling rate was set to 10 s. The monitoring points were assessed every six months from September 2012 to September 2016. Finally, eight set of time frame monitoring data were acquired. The data were interpolated by kriging and the grid graphics of the vertical displacement contour lines are illustrated in Fig. 5. The surface subsidence area of the Xishan gold mine occurs in the hanging wall surface corresponding to the stope. The footwall surface does not exhibit obvious subsidence deformation and may even be slightly uplifted owing to the effect of beams on the elastic

**Fig. 4** Distribution of monitoring points in the Xishan gold mine



foundation. The vertical displacement contour lines are more dense near fault F1. The maximum ground settlement is 329.26 mm.

**OLS model results**

From the results of the exploratory analysis, the coefficient, probability and variance inflation factor (VIF) values listed in Table 2 were obtained. The VIF is a test of multicollinearity among data and its values greater than 7.5 indicate that variables are redundant (Jan Blachowski 2016). The selected variables had low VIF values. The vertical displacement exhibited positive correlations with the surface slope, slope aspect, thickness of gold deposits, and depth below the ground of gold deposits, and a negative correlation with the digital elevation model of the surface. Figure 6 represents the map of standardized residuals in the OLS model. The R2 and the AICc are statistics derived from the regression equation to quantify model performance. R-squared is a measure of goodness of fit. Its value varies from 0.0 to 1.0, with higher values being preferable. It may be interpreted as the proportion of dependent variable variance accounted for by the regression model. AICc is a measure of model performance and is helpful for comparing different regression models. Taking into account model complexity, the model with the lower AICc value provides a better fit to the observed data. AICc is not an absolute measure of goodness of fit but is useful for comparing models with different explanatory variables as long as they apply to the same dependent variable. If the AICc values for two models differ by more than three, the model with the lower AICc is held to be better. Comparing the GWR

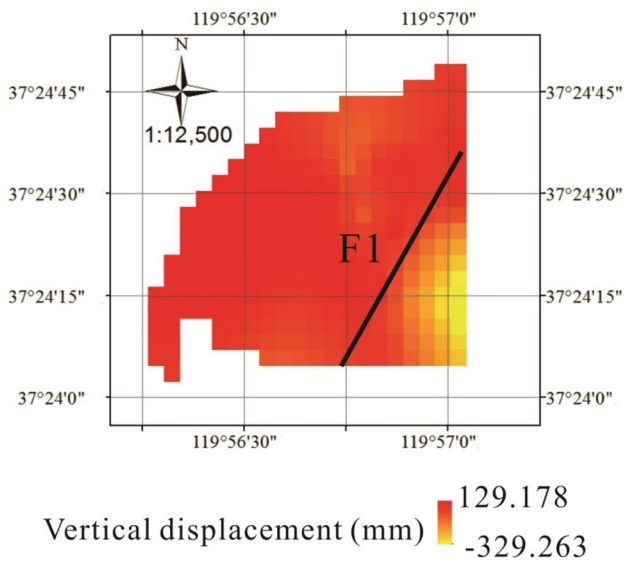


Fig. 5 Grid graphics of vertical displacement contour lines

AICc value to the OLS AICc value is one way to assess the benefits of moving from a global model (OLS) to a local regression model (GWR). The value of R<sup>2</sup> statistic is equal to 0.39 and the lowest value of the Akaike information criterion (AICc) statistic is equal to 10931.42. It is generally recognized that greater R<sup>2</sup> and smaller AICc values indicate that a model is rational. For the OLS model, the R<sup>2</sup> value is too low and the AICc value is too high; thus, a more advanced GWR model should be applied.

**GWR model results**

The same independent variables were used to construct a GWR model. The results are summarized in Table 3. As seen from the table, the statistic of the GWR model equal to 0.82 in comparison with 0.39 was obtained in the OLS analysis. The AICc value of GWR model was 7094.74 in comparison with 10931.42 obtained in the OLS analysis. Greater R<sup>2</sup> and smaller AICc values indicate that the GWR

Table 2 Summary of the OLS statistic

Independent variables	Coefficient	Probability	VIF
Digital elevation model of the surface	- 0.098181	0.000018	1.347293
Surface slope	0.422151	0.000001	1.327217
Slope aspect	0.014444	0.0455945	1.07112
Thickness of gold deposits	0.211246	0.00002	3.831661
Depth of gold deposits below the ground	0.050228	0.059544	3.763722

Fig. 6 Map of standardized residuals in the OLS model

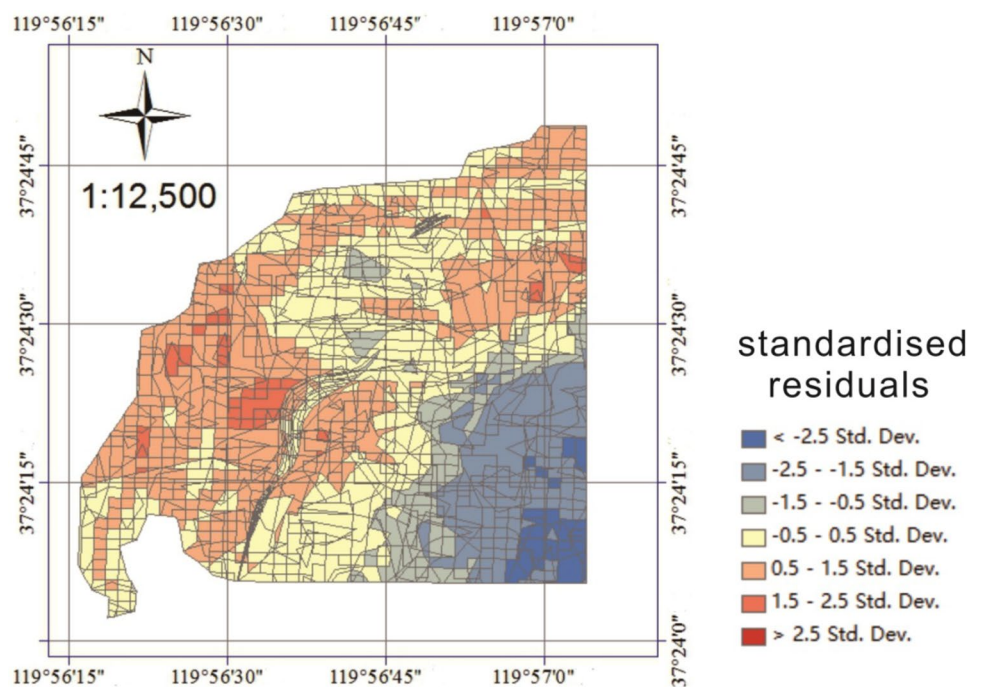
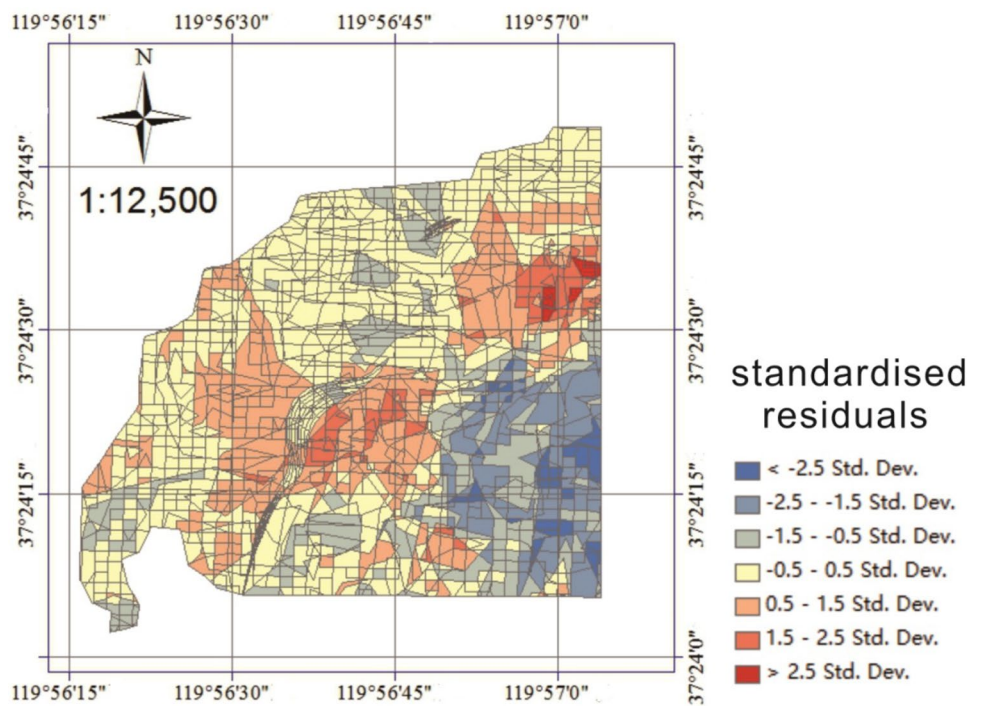


**Table 3** Results of the GWR model

Object ID	Varname	Variable	Definition
1	Bandwidth	390.8867425	
2	Residual squares	2391.37	
3	Effective number	28.17658324	
4	Sigma	0.976505394	
5	AICc	7094.74	
6	$R^2$	0.819287371	
7	$R^2$ adjusted	0.817329039	
8	Dependent field	0	Vertical displacement
9	Explanatory field	1	Digital elevation model of the surface
10	Explanatory field	2	Depth of gold deposits below the ground
11	Explanatory field	3	Surface slope
12	Explanatory field	4	Slope aspect
13	Explanatory field	5	Thickness of gold deposits

**Fig. 7** Map of standardized residuals in the GWR model

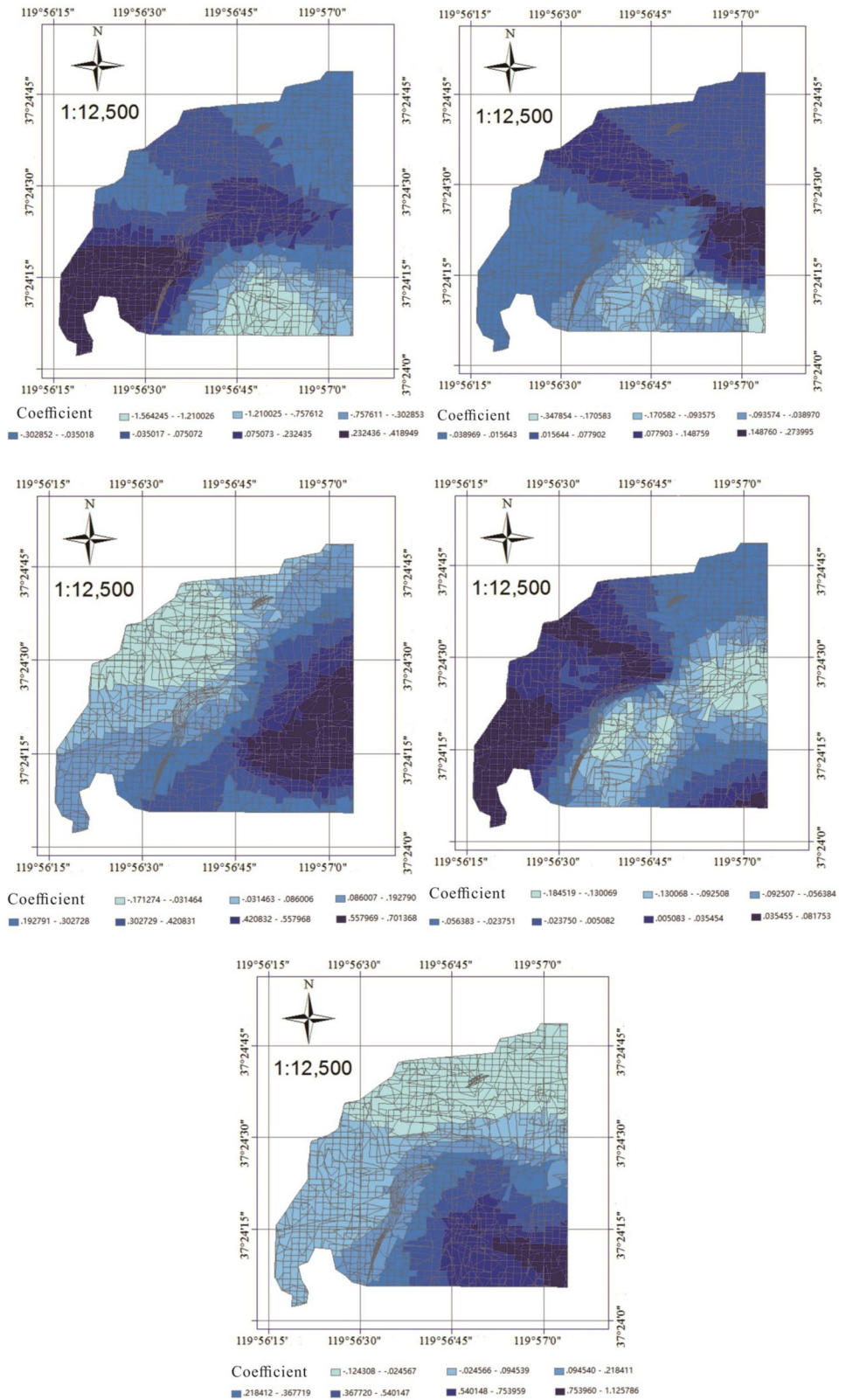


model is superior to the global regression model. So, we can say the GWR model has captured the spatial heterogeneity of independent variables. Figure 7 contains the map of standardized residuals in the GWR model. Figure 8 shows maps of coefficients for the independent variables (the digital elevation model of the surface, depth below the ground of gold deposits, surface slope, slope aspect, and thickness of gold deposits). The accuracy of the subsidence value in the area used for validation is  $\pm 8.5$  mm with a maximum calculated subsidence of  $-329.26$  mm. In conclusion, the GWR model is reliable.

**Prediction of seabed subsidence of the Xinli gold mine**

Traditional GPS measurement method cannot monitor seabed subsidence, hence, the OLS model cannot meet the accuracy requirements. Accordingly, the GWR model was used to predict the seabed subsidence of the Xinli gold mine. The prediction model was constructed using the ArcGIS model builder. The entire process is shown in Fig. 9. Information on the study area was incorporated into the verified GWR model, then regression was carried out to produce the predicted results. As the terrain conditions of the seabed cannot be measured, it was assumed that the seabed is almost

**Fig. 8** Map of coefficient for independent variables in the GWR model



level and gradually becomes steeper from east to west. The predicted results are shown in Fig. 10. The maximum subsidence area is located in the northeast corner of the mine,

which is at the surface corresponding to the hanging wall of the ore body. There is no obvious inhomogeneous subsidence: the minimum subsidence is 45.2 mm, the maximum is



**Fig. 9** Flowchart for the GWR model

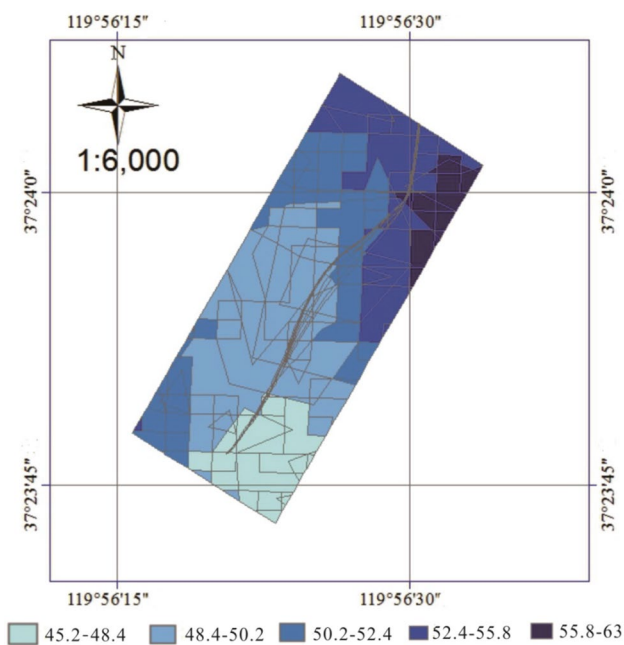
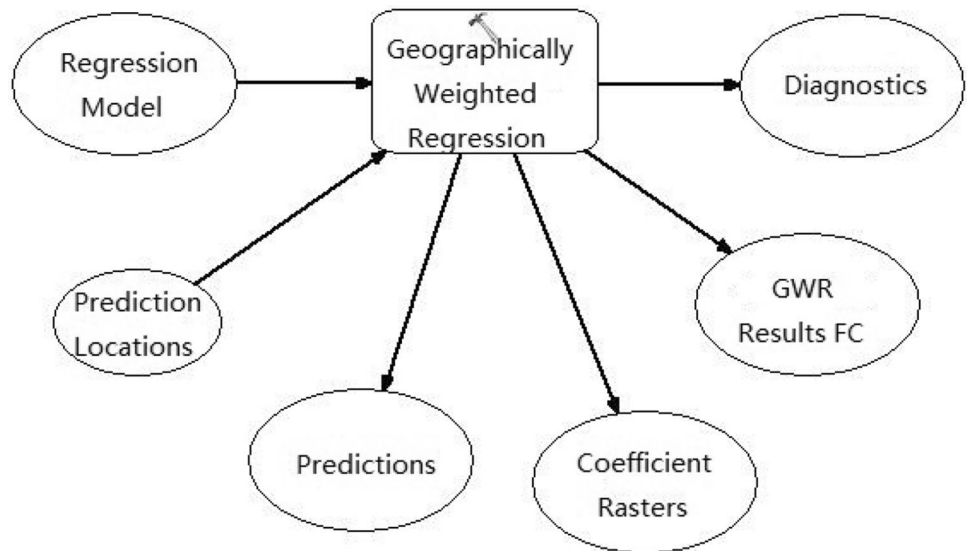


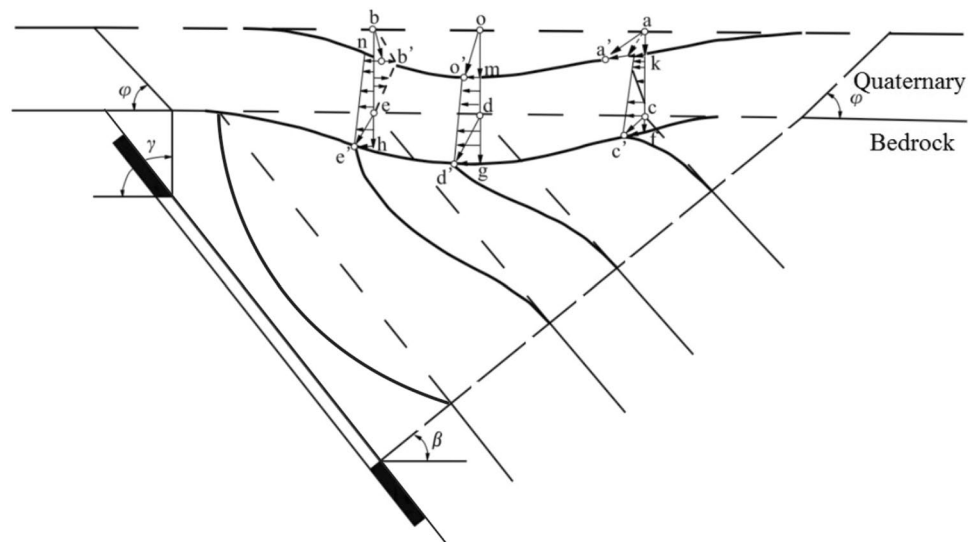
**Fig. 10** Predicted results from the GWR model

63 mm, and the average subsidence is – 50 mm. Therefore, it can be concluded that at present the Xinli gold mine is stable and will not experience a water inrush accident caused by inhomogeneous subsidence.

There is a general rule that metal mines often develop a discontinuous surface that is consistent with the best-developed faults in the surrounding rock of the ore body. The normal stress and the shear strength on the discontinuity surface decreased after excavation, causing activation of the discontinuity surface. The activated discontinuity surface will increase the stress field intensity factor near a crack

tip. The compliance of the rock mass is proportional to the square of the stress field intensity factor. As the compliance of the rock mass decreases, the rock mass movement range increases and the rock mass moves to the goaf. As the bedrock is covered by a loose sedimentary layer, the movement of bedrock determines the movement of the sedimentary layer. When the bedrock is horizontal or approximately level (i.e.,  $\alpha < 8^\circ$ ), the movement of the sedimentary layer is exactly the same as the movement of the underlying bedrock, which is basically a form of vertical bending. When the bedrock is cut into inclined rock mass by the discontinuity surface, the movement of the sedimentary layer is different from that of the bedrock. In this situation, the movement of the sedimentary layer is composed of two parts, vertical bending and horizontal dislocation in the uphill direction of the rock mass. The combination of these two movements causes the horizontal movement of the sedimentary layer to be complicated. In Fig. 11c, d, e the position of the points on the bedrock before movement is indicated, and  $c'$ ,  $d'$ , and  $e'$  indicate the position after moving. The moving vectors are  $\overline{cc'}$ ,  $\overline{dd'}$ , and  $\overline{ee'}$ , and the components of horizontal movement are  $\overline{fc'}$ ,  $\overline{gd'}$ , and  $\overline{he'}$ . The horizontal component of movement decreases gradually from the bottom to the top of the sedimentary layer. Similarly, if the surface has three points  $a$ ,  $o$ , and  $b$ , and point  $o$  is the center of ground subsidence, then when the rock layer bends vertically downward, the horizontal displacement component of the surface points is approximately symmetrical with respect to point  $o$ . The horizontal displacement of point  $o$  is zero, and the horizontal displacements of points  $a$  and  $b$  are in the direction of point  $o$ . In contrast, when the bedrock is affected by a discontinuity surface, the three points ( $a$ ,  $o$ , and  $b$ ) will be affected by two kinds of horizontal movement. The horizontal displacement of point  $a$  is the sum of the two horizontal

**Fig. 11** Movement and rock deformation caused by mining of an inclined ore body



movements, the horizontal displacement of point *b* is the difference between the two, and point *o* experiences uphill horizontal dislocation. Therefore, the horizontal movement in the surface movement basin is asymmetrical, that is, the horizontal movement increases in the uphill direction and decreases in the downhill direction. Because of the overlapping effect of the Xishan gold mine, the subsidence center of the Xinli mining area will move to the Xishan mining area and the subsidence center will be in the northeastern corner of the mining area, as shown in Fig. 10.

## Conclusions

The Xinli mining area of the Sanshandao gold mine contains a submarine deposit. The key point is that there is no inhomogeneous subsidence, cracking and subsidence in exploitation of the seabed. As the Xinli and Xishan gold mines are similar in their engineering geological conditions, ore body occurrence, and mining method, a GIS-based multifactorial weighted spatial regression approach was used to develop a spatial model of subsidence in the Xishan gold mine. The spatial model was applied to predict the mining-caused seabed subsidence in the Xinli gold mine. The main conclusions are:

1. The vertical displacement shows a positive correlation with the surface slope, slope aspect, thickness of gold deposits, and depth of gold deposits below the ground, and a negative correlation with the digital elevation model of the surface.
2. For the OLS model, the  $R^2$  value was 0.39, which is not sufficiently high to meet the needs of research. Thus, a more advanced GWR model was used in the analysis.

3. The GWR model captured the spatial heterogeneity of the independent variables, with  $R^2=0.82$ .
4. The verified GWR model to predict the seabed subsidence in the Xinli gold mine yields the result that there is no obvious inhomogeneous subsidence of the seabed, and the average subsidence is  $-50$  mm.
5. When the bedrock is cut into inclined rock mass by the discontinuity surface, the horizontal movement in the surface movement basin is asymmetrical, that is, the horizontal movement increases in the uphill direction and decreases in the downhill direction. Because of the overlapping effect of the Xishan gold mine, the subsidence center of the Xinli mining area will move to the Xishan mining area and the subsidence center will be in the northeastern corner of the mining area.

**Acknowledgements** The research was supported by the National Natural Science Foundation of China (Grant nos. 41831293, 41772341). Grateful appreciation is expressed for the support.

## References

- Blachowski J (2016) Application of GIS spatial regression methods in assessment of land subsidence in complicated mining conditions: case study of the Walbrzych coal mine (SW Poland). *Nat Hazards* 84:997–1014
- Coal Industry Promotion Board, CIPB (1997) A study on the Mechanism of subsidence over abandoned mine area and the construction method of subsidence prevention. Coal Industry Promotion Board, Seoul, 97-06:1–67
- Dolezalova H, Kajzar V, Soucek K, Stas L (2009) Evaluation of mining subsidence using GPS data. *Acta Geodyn Geomater* 6(3):359–367
- Dolezalova H, Kajzar V, Soucek K, Stas L (2012) Analysis of surface movements from undermining in time. *Acta Geodyn Geomater* 9(3):389–400

- Foster AS, Gorr WL (1986) An adaptive filter for estimating spatially varying parameters: application to modeling police hours spent in response to calls for service. *Manag Sci* 32(7):878–889
- Fotheringham AS, Brunson C, Charlton M (1998) Geographically weighted regression: a natural evolution of the expansion method for spatial data analysis. *Environ Plan A* 30(11):1905–1927
- Gorr WL, Olligshlaeger AM (1994) Weighted spatial adaptive filtering: Monte Carlo studies and application to illicit drug market modeling. *Geogr Anal* 26:67–87
- Missavage RJ, Chugh YP, Roscetti T (1986) Subsidence prediction in shallow room and pillar mines. *Int J Min Geol Eng* 4:39–46
- Nestbitt A (2003) Subsidence monitoring West Cliff Colliery long-wall 5A4. APAS (Association of Public Authority Surveyors) 2003 Conference, Wollongong, Australia, 1–4 April, 133–139
- Sahu SP, Yadav M, Das AJ et al (2017) Multivariate statistical approach for assessment of subsidence in Jharia coalfields, India. *Arab J Geosci* 10:191
- Siriwardane HJ, Amanat J (1986) Analysis of mining subsidence caused by underground mining. *Int J Min Eng* 2:271–290
- Waltham AC (1989) Ground subsidence. Blackie & Son Ltd, New York, pp 49–97
- Wu S, Yu Z, Zhou D, Zhang H (2006) Structural features and Cenozoic evolution of the Tan-Lu fault zone in the Laizhou Bay, Bohai Sea. *Mar Geol Quat Geol* 26:101–110

**Publisher's Note** Springer Nature remains neutral with regard to jurisdictional claims in published maps and institutional affiliations.